Incomplete fusion studies in the $^{19}F + ^{159}Tb$ system at low energies and its correlation with various systematics

Mohd. Shuaib,[1,*] Vijay R. Sharma,[1] Abhishek Yadav,[2] Pushpendra P. Singh,[3] Manoj Kumar Sharma,[4] Devendra P. Singh,[5] R. Kumar,[2] R. P. Singh,[2] S. Muralithar,[2] B. P. Singh,[1,†] and R. Prasad[1]

[1]*Nuclear Physics Laboratory, Physics Department, A. M. U, Aligarh-202 002, India*

[2]*NP-Group, Inter-University Accelerator Centre, New Delhi-110 067, India*

[3]*Department of Physics, Indian Institute of Technology Ropar, Punjab-140 001, India*

[4]*Physics Department, S. V. College, Aligarh-202 001, India*

[5]*Department of Physics, University of Petroleum and Energy Studies, Dehradun 248 007, India*

(Received 22 April 2016; published 21 July 2016)

The excitation functions of reaction residues populated via the complete fusion and incomplete fusion process in the interaction of the $^{19}F + ^{159}Tb$ system have been measured at energies $\approx$ 4–6 MeV/nucleon, using off-line γ-ray spectroscopy. The analysis of data was done within the framework of statistical model code PACE4 (a compound nucleus model). A significant fraction of incomplete fusion was observed in the production of reaction residues involving α particle(s) in the exit channels, even at energies as low as near the Coulomb barrier. The incomplete fusion strength function was deduced from the experimental excitation functions and the dependence of this strength function on various entrance channel parameters was studied. The present results show a strong dependence on the projectile α-Q value that agrees well with the existing data. To probe the dependence of incomplete fusion on entrance channel mass asymmetry, the present work was compared with the results obtained in the interaction of ^{12}C, ^{16}O, and ^{19}F with nearby targets available in the literature. It was observed that the mass asymmetry linearly increases for each projectile separately and turns out to be a projectile-dependent mass-asymmetry systematics. The deduced incomplete fusion strength functions in the present work are also plotted as a function of $Z_P Z_T$ (Coulomb effect) and compared with the existing literature. A strong dependence of the Coulomb effect on the incomplete fusion fraction was observed. It was found that the fraction of incomplete fusion linearly increases with $Z_P Z_T$ and was found to be more for larger $Z_P Z_T$ values indicating significantly important linear systematics.

DOI: 10.1103/PhysRevC.94.014613

I. INTRODUCTION

Continuous efforts have been made to understand the dynamics of heavy-ion (HI) [1–3] induced reactions in the recent decade at energies starting from near the Coulomb barrier to well above it (i.e., 4–7 MeV/nucleon). At these energies, the presence of incomplete fusion reactions has triggered the resurgent interest [4–11]. The complete fusion (CF) and incomplete fusion (ICF) processes, in general, can be disentangled on the basis of driving angular momenta (ℓ waves) [12,13], i.e., for the angular momenta value(s) $\ell < \ell_{\rm crit}$, (where $\ell_{\rm crit}$ is the critical angular momentum of the system) a completely fused composite system emerges because of the intimate contact and transient amalgamation of the entire projectile with the target nucleus. However, at relatively higher angular momenta values $\ell > \ell_{\rm crit}$, it is generally assumed that the projectile breaks into fragments in the vicinity of target nuclear field, to sustain the excess angular momentum, where a part of the projectile gets fused with the target nucleus and the remnant moves in the forward direction without any interaction. As a consequence, the fusion of the entire projectile is hindered and gives rise to the ICF process. The partial fusion of the incident projectile leads to an incompletely fused composite system with less charge, mass, and excitation energy. The first experimental evidence of projectilelike fragments (PLFs) emitted in such reaction processes was reported by Britt and Quinton [14]. The similar observations were reported at relatively low energies by Kauffmann and Wolfgang [15], where the PLFs were detected in the forward cone. The advancement in the particle-γ coincidence measurements done by Inamura *et al.* [16] and Zolnowski *et al.* [10,17,18] provide a proper window to understand the ICF reaction dynamics. Furthermore, Geoffroy *et al.* [19] measured the correlation between energies and angular distribution of charged particle(s) along with γ multiplicity, which indicates the origin of PLFs from undamped noncentral interactions. The review presented by Gerschel *et al.* [20] on ICF, suggested that the localization of the ℓ window depends on the target deformation. Recently, the localization of the ℓ window in ICF reactions was reported in the spin-distribution measurements as well [10,18].

To understand the reaction dynamics of ICF processes, various theoretical models have been developed and tested. The SUMRULE model of Wilczynski *et al.* [21] proposes the appearance of the ICF process as a result of peripheral interactions and are confined for the values of angular momenta (ℓ) above the critical value ($\ell_{\rm crit}$) for complete fusion. The break-up fusion (BUF) model [22–24] of Udagawa and Tamura is based on distorted wave Born approximation (DWBA), in which the projectile is assumed to break up into α clusters,

*shuaibphy67@gmail.com

†bpsinghamu@gmail.com

when it reaches within the nuclear field of the target nucleus. One of the fragments of the projectile fuses with the target nucleus to form an incompletely fused composite system while the remnant moves in the forward cone with the projectile velocity. In the promptly emitted particles model (PEPS) [25], the nucleons from the projectile are transferred to the target nucleus and get accelerated from the target nucleus field and acquire extra velocity to escape. It may be mentioned that the above mentioned reactions models have been able to explain to some extent the ICF data at energies > 10.5 MeV/nucleon but have completely failed to reproduce the experimental ICF data at lower energies $\approx$ 4–7 MeV/nucleon [9]. As such, there is no theoretical model valid for low energy ICF reactions.

The presence of ICF at low energies and its influence on CF raise many issues such as how does the degree of fusion incompleteness depend on (i) projectile energy, (ii) driving input angular momenta, (iii) mass asymmetry of the interacting partners, (iv) binding energy of the projectile, (v) projectile-target charge product (i.e., $Z_P Z_T$), and (vi) the α-Q value of the projectile; these need to be systematically explored. Systematic study of the above mentioned parameters is likely to help in the development/refinement of existing reaction models to explain ICF at low energies.

To understand the onset of ICF and its effect on CF as well as on various entrance channel parameters mentioned above, an experiment was performed at the Inter University Accelerator Center (IUAC), New Delhi, India. In the present work, the excitation function (EFS) of reaction residues populated in the ^{19}F + ^{159}Tb system are measured at energies $\approx$ 4–6 MeV/nucleon and are analyzed within the framework of statistical model code PACE4, [26]. The ICF strength function ($F_{\rm ICF}$) was extracted from the analysis of experimental EFS and compared with the existing literature as a function of various entrance channel parameters. The present work is also analyzed within the framework of recently proposed α-Q value systematics [27]. An attempt was made to find a systematics from the Coulomb effect ($Z_P Z_T$, where Z_P and Z_T are the atomic numbers of projectile and target, respectively). The present results indicate a strong dependence of incomplete fusion probability on Coulomb effect for the first time.

II. EXPERIMENTAL DETAILS

The experiment for the system ^{19}F+^{159}Tb was performed at the Inter University Accelerator Center (IUAC), New Delhi. The accelerated ion beam of $^{19}F^{7+}$ was produced via the 15UD-pelletron accelerator. The natural ^{159}Tb targets of thickness $\approx$ 1.2–2.5mg/cm^2 and aluminium-catcher foils of thickness $\approx$ 1.5–2.5 mg/cm^2 were prepared by using the rolling technique. The Al foils of suitable thickness have been used with the dual purpose of degrading the energy of the incident beam and also for catching the recoiling residues. The thickness of the target and catcher foils is measured by the α-transmission method, which is based on the energy loss per unit length by α particles having energy $\approx$ 5.487 MeV emitted from the standard ^{241}Am source. To cover a wide range of energy, an energy degradation technique was used in a single irradiation. Four stacks each consisting of three target-catcher foil assemblies were prepared and irradiations were carried out in the general purpose scattering chamber (GPSC) at energies $\approx$ 99.45 $\pm$ 1.54, 102.6 $\pm$ 1.40, 105.44 $\pm$ 1.56, and 108.1 $\pm$ 1.90 MeV. To minimize the time lapse between the stop time of irradiation and the beginning of the counting of the activity induced in the target-catcher foil assembly, an in-vacuum transfer facility was used. The energy of incident beam falling on the midpoint of each target is estimated by using code SRIM [28]. Considering the half lives of interest, the irradiations were carried out for $\approx$ 8–10 h of duration for each stack. A Faraday cup was installed behind the target-catcher foil assembly to determine the beam flux. The beam current during the experiment is maintained at $\approx$ 25–30 nA for all irradiations. The radioactivity induced in the target-catcher foil assemblies were recorded by a pre-calibrated high resolution HPGe detector coupled to a CAMAC-based data acquisition system [29]. The HPGe detector used in this experiment is calibrated using standard gamma sources viz., ^{60}Co, ^{137}Cs, ^{133}Ba, and ^{152}Eu. The efficiency of the detector was determined using the same source at various distances to wash out the solid angle effect. Reaction residues populated in the interaction of ^{19}F + ^{159}Tb have been identified by their characteristic γ lines, and confirmed by decay curve analysis. As a representative case, a typical γ-ray spectrum at incident laboratory energy $\approx$ 105.44 $\pm$ 1.56 MeV is shown in Fig. 1, and some of the γ peaks corresponding to different CF and/or ICF residues are marked. The production cross section of the reaction residues ($\sigma_{\rm ER}$) was determined using the standard formulation as described in Ref. [14]. In the present work, the overall possible error including statistical errors are estimated to be $\leqslant$ 15%, excluding the uncertainty in branching ratio, decay constants, etc., which have been taken from the Table of Radioactive Isotopes [30].

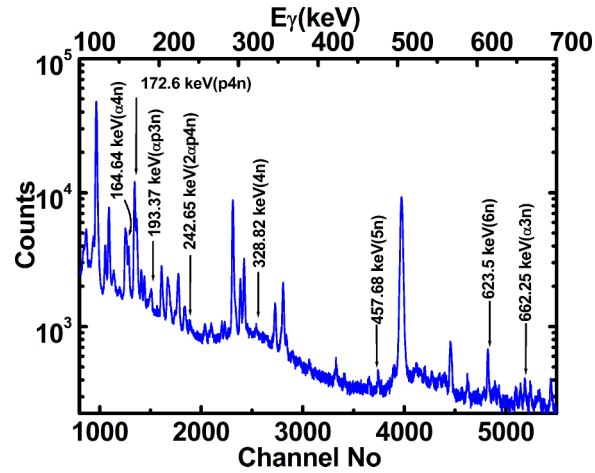

FIG. 1. Typical gamma ray spectrum of ^{19}F+^{159}Tb interaction at energy $\approx$ 105.44 $\pm$ 1.56 MeV, where γ lines are assigned to different reaction products expected to be populated by complete fusion and/or incomplete fusion processes.

III. ANALYSIS AND INTERPRETATION OF DATA

The EFS of various reaction residues populated via CF and/or ICF modes in ^{19}F + ^{159}Tb system have been measured

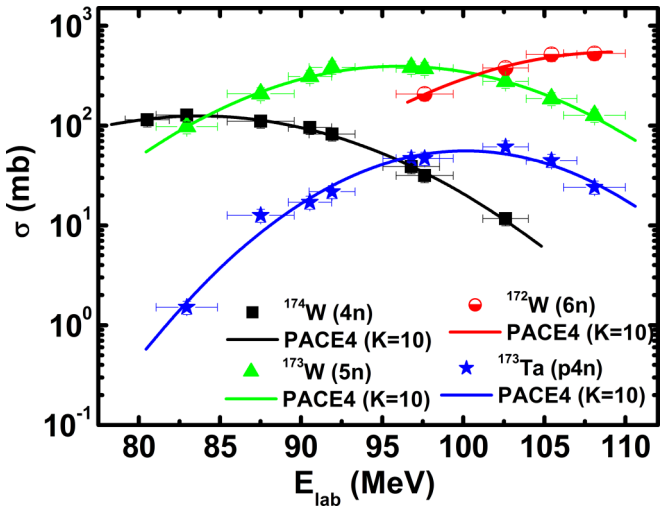

FIG. 2. Experimentally measured excitation functions of all xn/pxn channels populated in the ^{19}F + ^{159}Tb system. The solid lines through the experimental data points are the PACE4 calculations as discussed in the text.

at energies $\approx$ 81–110 MeV and are analyzed within the framework of statistical model code PACE4 [26]. A detailed description and listing of input parameters of this code are presented elsewhere [26,27,31–33]. It may be pertinent to mention here, that PACE4 computes only the CF events according to the Hauser-Feshbach theory of CN decay, and it does not include the transfer and/or ICF channels. Therefore, any deviation in the experimental EFS with respect to the theoretical calculations based on PACE4 may be attributed to the ICF process. In this code, the nuclear level density parameter (a = A/K) plays an important role, which is used to reproduce the experimental EFs.

Figure 2 shows the experimental EFS of ^{174}W, ^{173}W, ^{172}W, and ^{173}Ta residues populated via 4n, 5n, 6n, and p4n emission, respectively, and compared with the corresponding PACE4 calculations. During the decay curve analysis, the radionuclides ^{173}Ta(p4n) are found to be strongly fed from its higher charge isobar (precursor hereafter) ^{173}W(5n) through β^+ emission. Therefore, the independent cross section ($\sigma_{\rm ind}$) of ^{173}Ta residues was deduced by using the successive radioactive decay formulations presented in Ref. [34]. As can be seen from this figure, the theoretical calculations of PACE4 are found to be best fitted to the experimental EFs for the level density parameter a = A/10 MeV^{-1}. As may be seen from Fig. 2, the theoretical PACE4 calculations for the channels (4n, 5n, 6n, and p4n) agree reasonably well with the experimental measurements indicating that these channels are populated via the CF process.

To figure out if the α-emitting channels are populated via CF and/or ICF processes, the sum of experimental EFs of all identified α-emitting channels [$\sum \sigma_{\alpha xn+\alpha pxn+2\alpha xn+2\alpha pxn}$(exp), i.e., the sum of the cross section of ^{171,170}Hf(αxn), ^{170}Lu(αpxn), ^{167}Yb($2\alpha xn$), ^{167,165}Tm($2\alpha pxn$) residues] was compared with that estimated by corresponding PACE4 calculations and are presented in Fig. 3(a). The calculations of EFs for these α-emitting channels have been performed consistently using

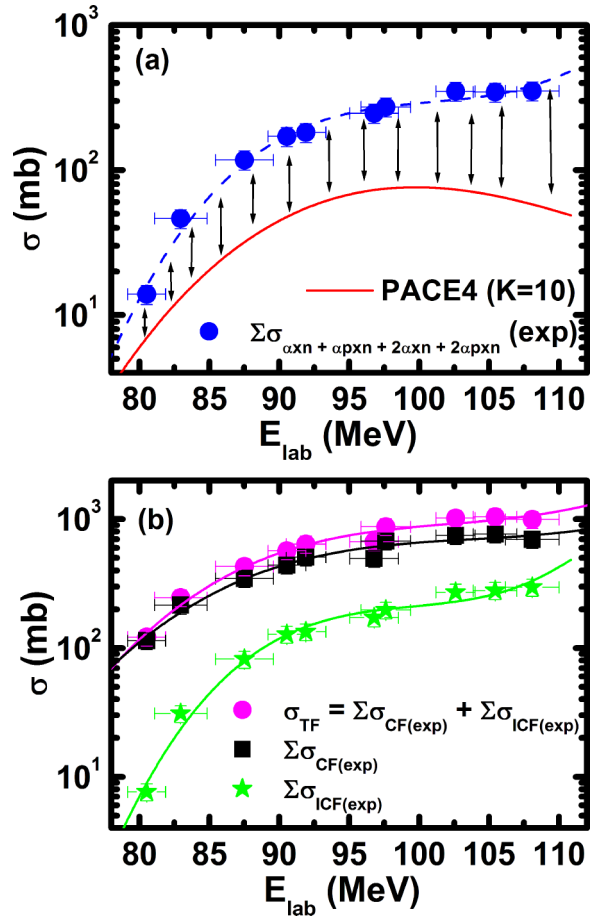

FIG. 3. (a) Sum of experimentally measured excitation functions of all α-emitting channels compared with the predictions of corresponding statistical model code PACE4. The line through the blue dot points is drawn to guide the eyes. (b) Comparison of $\sigma_{\rm TF}$, $\sigma_{\rm CF}$, and $\sigma_{\rm ICF}$ cross sections for the ^{19}F + ^{159}Tb system with the incident laboratory energy. The lines are drawn to guide the eyes.

the same set of input parameters, which have been used to reproduce the EFs of xn/pxn channels. As can be seen from Fig. 3(a), the experimental EFs for α-emitting channels are significantly higher than the predictions of statistical model code PACE4. This observed enhancement in the experimental EFs of α-emitting channels may be attributed to the contribution of the ICF process in the production of these residues.

The contribution of the ICF cross section in the production of α-emitting channels is deduced according to the formulation $\sigma_{\rm ICF} = \sum \sigma_{\rm exp}^{\alpha's}$ - $\sum \sigma_{\alpha's}^{\rm PACE4}$ [27,33] at each energy. To see the the influence of ICF in the total reaction cross section, the ($\sigma_{\rm TF}$ = $\sum \sigma_{\rm CF(exp)}$ + $\sum \sigma_{\rm ICF(exp)}$), was obtained and plotted with $\sum \sigma_{\rm CF(exp)}$ (sum of all xn and $p$xn channels) as a function of projectile energy in Fig. 3(b). From this figure, the onset of ICF is clearly evident at energies as low as $\approx$ 80 MeV (i.e., 8% above the barrier) and increases as the incident energy increases.

To get a proper visualization into the onset and strength of ICF, the incomplete fusion strength function $F_{\rm ICF}$, was extracted from the data presented in Fig. 3(b). The $F_{\rm ICF}$ is defined as the empirical probability of ICF at different projec-

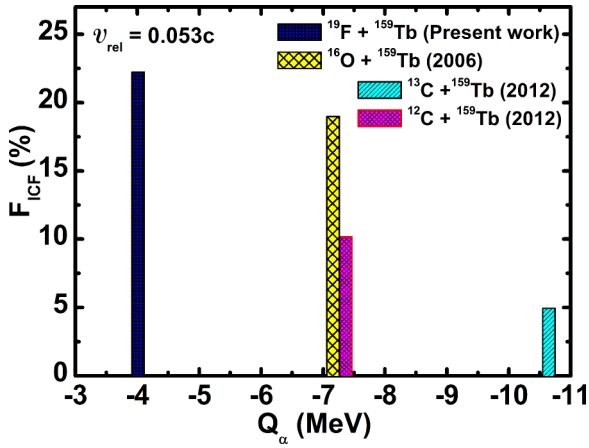

FIG. 4. A comparison of incomplete fusion strength function ($F_{\rm ICF}$) in terms of the α-Q value of the projectile at a constant $v_{\rm rel}$ (= 0.053c) for different projectiles on the same target ^{159}Tb. The data were taken from Ref. [27].

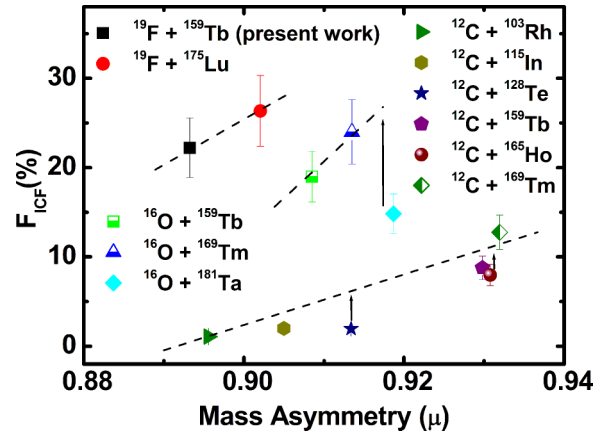

FIG. 5. Incomplete fusion strength function ($F_{\rm ICF}$) of various systems (see text) as a function of mass asymmetry (μ). The dashed lines are drawn to guide the eyes.

tile energies and can be expressed as $F_{\rm ICF}(\%) = (\sum \sigma_{\rm ICF}/\sigma_{\rm TF}) \times 100$. To have better understanding about the effect of projectile structure dependence on ICF, the deduced $F_{\rm ICF}$ values are analyzed within the framework of recently proposed α-Q value systematics [27] and compared with that available in the literature (see Ref. [33] for details), and shown in Fig. 4. It is evident from this figure that the percentage ICF fraction is found to be more for the less negative α-Q value of the ^{19}F projectile and significantly decreases as the α-Q value becomes more negative for ^{16}O, ^{12}C, and ^{13}C projectiles. A projectile with a large negative α-Q value is strongly bound (less break-up probability into the α cluster) as compared to the projectile with relatively less negative α-Q value. Hence, the break-up probability of the ^{19}F projectile ($Q_\alpha = -4.48$ MeV) into the α cluster is expected to be more as compared to projectiles with more negative α-Q values, i.e., ^{16}O, ^{12}C, and ^{13}C. From the data presented in Fig. 4, it can be inferred that the α-Q value is an important entrance channel parameter, which determines the ICF probability. The present results are found to be in good agreement with the systematics presented in Ref. [27]

To see how ICF depends on entrance channel mass asymmetry (μ), the present data are also analyzed within the framework of Morgenstern's *et al.* [35] systematics, i.e., the ICF significantly contribute above $v_{\rm rel} \approx 0.06c$ (6% of c), for more mass-asymmetric systems. Therefore, to test the Morgenstern's systematics [35], the value of $F_{\rm ICF}$ in the ^{19}F + ^{159}Tb system (present work) was deduced and compared with that obtained for ^{12}C + ^{103}Rh, ^{12}C + ^{115}In, ^{12}C + ^{128}Te, ^{12}C + ^{159}Tb, ^{12}C + ^{165}Ho, ^{12}C + ^{169}Tm (see Ref. [33] for details), ^{16}O + ^{159}Tb, ^{16}O + ^{169}Tm, ^{16}O + ^{181}Ta (see Ref. [27] for details), and ^{19}F + ^{175}Lu [36] systems at constant relative velocity $v_{\rm rel} = 0.053$c as a function of entrance channel mass asymmetry and presented in Fig. 5. As can be seen from this figure, the ICF strength function ($F_{\rm ICF}$) shows a systematic linear growth separately for each projectile (i.e., ^{12}C, ^{16}O, and ^{19}F) with different targets when mass asymmetry increases. In general, the probability of ICF increases with entrance channel mass asymmetry separately with different magnitudes for each projectile. However, the value of $F_{\rm ICF}$ for ^{16}O + ^{181}Ta system is slightly away from the increasing trend shown with the straight line. It may be because of the fact that in the case of the ^{16}O + ^{181}Ta system, all the α-emitting channels could not be measured [27] because of their short half-lives and/or very low γ-ray intensities. The present value of $F_{\rm ICF}$ for the ^{16}O + ^{181}Ta system is expected to go up (upward arrow in Fig. 5), if all possible α-emitting channels are measured. Further, the magnitude of $F_{\rm ICF}$ for systems with the same mass asymmetry (μ) and different projectiles are very different. As such, the present observation based on several projectile-target combinations indicates that $F_{\rm ICF}$ increases almost linearly with mass asymmetry for each projectile but with substantially different magnitudes. This observation is in contrast to the trend proposed by Morgenstern *et al.* [35], who predicted that ICF depends on the degree of mass symmetry in the entrance channel. As such, the present analysis may indicate a projectile-dependent mass-asymmetry trend rather than a simple rise with mass asymmetry. This is an important experimental observation and may be useful for the prediction of incomplete fusion contribution.

The onset and strength of ICF is also investigated in terms of the charge product of the projectile target (i.e., the product $Z_P Z_T$, where Z_P and Z_T are the atomic numbers of projectile and target nuclei, respectively). The deduced ICF strength function ($F_{\rm ICF}$) for the present work at the same constant relative velocity ($v_{\rm rel} = 0.053c$) is plotted as a function of $Z_P Z_T$ and is presented in Fig. 6. To strengthen the present result, the $F_{\rm ICF}$ for the system ^{19}F + ^{159}Tb (present work) is compared with that obtained for other systems available in the literature (see Refs. [27,33,36] for details).

As can be seen from this figure, the percentage of incomplete fusion fraction $F_{\rm ICF}$, follows a systematic linear growth, when the charge product $Z_P Z_T$ increases, and is found to be more for larger $Z_P Z_T$ values. In a more elaborative way, the experimental data fall on a straight line that increases with the increase in the value of the product $Z_P Z_T$, irrespective of the projectile-target combinations. As such, it may be prodigious

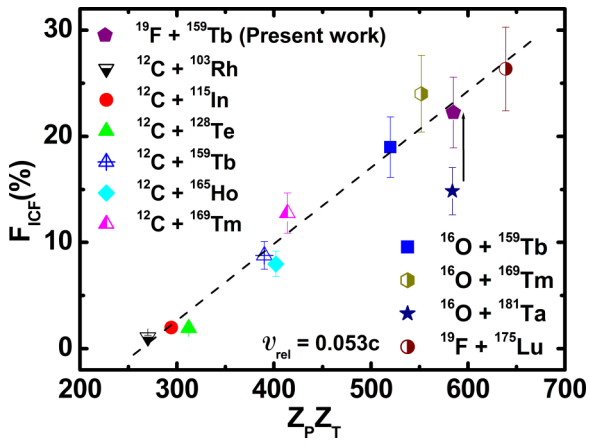

FIG. 6. Incomplete fusion strength function (F_{ICF}) of various systems (see text) as a function of $Z_P Z_T$. The dashed line is drawn to guide the eyes.

to point out that, as the projectile comes near the field of the target nucleus it may break up as a result of Coulomb interaction followed by the fusion of one of the fragments with the target nucleus. An increase in the value of $Z_P Z_T$ enhances the strength of the Coulomb interaction resulting in the larger break-up probability. This Coulomb effect systematics may help in proper modeling for ICF reactions. To the best of our knowledge, the linear dependence of the ICF fraction on the product $Z_P Z_T$ (Coulomb effect) was observed for the first time and may be used as a reliable parameter for further study and modeling of ICF at low energies.

IV. SUMMARY AND CONCLUSIONS

The probability of ICF was measured in the ^{19}F + ^{159}Tb system at low energies from the analysis of experimental EFs within the framework of statistical model code PACE4. A systematic study of the ICF fraction was performed as a function of various entrance channel parameters. In terms of α-Q value systematics [27], it was found that the ICF strongly depends on the projectile structure and suggests more ICF fraction for less negative α-Q value of the projectile (i.e., ^{19}F) and is found to be in good agreement with existing data [27]. In terms of entrance channel mass asymmetry, the present results indicate that the ICF strength increases almost linearly with the mass asymmetry but separately for each projectile. This is at variance with the observation of Morgenstern *et al.*'s, systematics [35], which suggested that ICF strongly depends on the degree of mass asymmetry. In the present work, a strong dependence of incomplete fusion strength function (F_{ICF}) on the Coulomb effect, i.e., $Z_P Z_T$, was observed for the first time. Further measurements involving the same CN for different projectile-target combinations may give insight to Coulomb effects. We plan to perform further investigations in this direction.

ACKNOWLEDGMENTS

The authors thank the director of IUAC, New Delhi and the chairperson of Department of Physics, A. M. U, Aligarh for providing all the necessary facilities to carry out this work. M.S., R.P., B.P.S., and V.R.S. thank the Department of Science & Technology, Government of India for Project No. SR/S2/HEP-30/2012 for financial support.

[1] F. Schussler, H. Nifenecker, B. Jakobsson, V. Kopljar, K. Söderström, S. Leray, C. Ngô, S. Souza, J. P. Bondorf, and K. Sneppen, Nucl. Phys. A **584**, 704 (1995).
[2] E. Gadioli, C. Brattari, M. Cavinato *et al.*, Nucl. Phys. A **641**, 271 (1998).
[3] S. Gupta, B. P. Singh, M. M. Musthafa, H. D. Bhardwaj, and R. Prasad, Phys. Rev. C **61**, 064613 (2000).
[4] A. Diaz-Torres and I. J. Thompson, Phys. Rev. C **65**, 024606 (2002); Phys. Rev. Lett. **98**, 152701 (2007).
[5] E. Z. Buthelezi *et al.*, Nucl. Phys. A **734**, 553 (2004).
[6] P. R. S. Gomes, I. Padron *et al.*, Phys. Rev. C **73**, 064606 (2006); Phys. Lett. B **601**, 20 (2004).
[7] M. Dasgupta *et al.*, Nucl. Phys. A **787**, 144 (2007).
[8] Pushpendra P. Singh *et al.*, Phys. Lett. B **671**, 20 (2009); Phys. Rev. C **80**, 064603 (2009); **78**, 017602 (2008).
[9] P. P. Singh, B. P. Singh, M. K. Sharma, Unnati, D. P. Singh, R. Prasad, R. Kumar, and K. S. Golda, Phys. Rev. C **77**, 014607 (2008) and references therein.
[10] P. P. Singh, M. K. Sharma, Unnati, D. P. Singh, Rakesh Kumar, K. S. Golda, B. P. Singh, and R. Prasad, Eur. Phys. J. **34**, 29 (2007).
[11] Unnati Gupta, P. P. Singh, D. P. Singh, M. K. Sharma, A. Yadav, R. Kumar, B.P. Singh, and R. Prasad, Nucl. Phys. A **811**, 77 (2008).
[12] M. Dasgupta, P. R. S. Gomes, D. J. Hinde *et al.*, Phys. Rev. C **70**, 024606 (2004).
[13] L. F. Canto, R. Donangelo, L. M. deMatos, M. S. Hussein, and P. Lotti, Phys. Rev. C **58**, 1107 (1998).
[14] H. C. Britt and A. R. Quinton, Phys. Rev. **124**, 877 (1961).
[15] R. Kauffmann and R. Wolfgang, Phys. Rev. **121**, 206 (1961).
[16] T. Inamura, M. Ishihara *et al.*, Phys. Lett. B **68**, 51 (1977); T. Inamura, A. C. Kahler, D. R. Zolnowski, U. Garg, T. T. Sugihara, and M. Wakai, Phys. Rev. C **32**, 1539 (1985).
[17] D. R. Zolnowski, H. Yamada, S. E. Cala, A. C. Kahler, and T. T. Sugihara, Phys. Rev. Lett. **41**, 92 (1978).
[18] Vijay R. Sharma, Pushpendra P. Singh, and Mohd. Shuaib *et al.*, Nucl. Phys. A **946**, 182 (2016).
[19] K. A. Geoffroy, D. G. Sarantites, M. L. Halbert, D. C. Hensley, R. A. Dayras, and J. H. Barker, Phys. Rev. Lett. **43**, 1303 (1979).
[20] C. Gerschel, Nucl. Phys. A **387**, 297 (1982).
[21] J. Wilczynski *et al.*, Nucl. Phys. A **373**, 109 (1982).
[22] T. Udagawa, D. Price, and T. Tamura, Phys. Rev. Lett. **45**, 1311 (1980).
[23] T. Udagawa, D. Price, T. Tamura *et al.*, Phys. Lett. B **116**, 311 (1982).
[24] E. Takada, T. Shimoda, N. Takahashi, T. Yamaya, K. Nagatani, T. Udagawa, and T. Tamura, Phys. Rev. C **23**, 772 (1981).

[25] J. P. Bondrof, J. N. De, G. Fái, A. O. T. Karvinen, B. Jakobsson, and J. Randrup, Nucl. Phys. A. **333**, 285 (1980).
[26] A. Gavron, Phys. Rev. C **21**, 230 (1980).
[27] V. R. Sharma, A. Yadav, P. P. Singh, D. P. Singh, S. Gupta, M. K. Sharma, I. Bala, R. Kumar, S. Murlithar, B. P. Singh, and R. Prasad, Phys. Rev. C **89**, 024608 (2014) and references therein.
[28] Computer code "The Stopping and Range of Ions in Matter" (SRIM): [http://www.srim.org/SRIM/SRIMLEGL.htm].
[29] CANDLE-Collection and Analysis of Nuclear Data using Linux Network, B. P. Ajith Kumar *et al.*, DAE **SNP**, 2001, Kolkatta.
[30] E. Browne and R. B. Firestone, *Table of Radioactive Isotopes* (Wiley, New York, 1996).
[31] R. Bass, Nucl. Phys. A **231**, 45 (1974).
[32] F. D. Becchetti and G. W. Greenless, Phys. Rev. **182**, 1190 (1969).
[33] Abhishek Yadav *et al.*, Phys. Rev. C **85**, 034614 (2012).
[34] M. Cavinato, E. Fabrici, E. Gadioli, E. GadioliErba, P. Vergani, M. Crippa, G. Colombo, I. Redaelli, and M. Ripamonti, Phys. Rev. C **52**, 2577 (1995).
[35] H. Morgenstern, W. Bohne, W. Galster, K. Grabisch, and A. Kyanowski, Phys. Rev. Lett. **52**, 1104 (1984); Z. Phys. A **313**, 39 (1983); Phys. Lett. B **113**, 463 (1982).
[36] Abhay V. Agarwaal, Vijay R. Sharma, Mohd. Shuaib *et al.*, Proceedings of the DAE-BRNS Symp. on Nucl. Phys. **60**, 470 (2015).